

# In-medium Properties of Hadrons – Observables II

L. Alvarez-Ruso, T. Falter, U. Mosel, P. Muehlich  
Institut fuer Theoretische Physik, Universitaet Giessen  
D-35392 Giessen, Germany

November 10, 2018

## Abstract

In this review we discuss the observable consequences of in-medium changes of hadronic properties in reactions with elementary probes, and in particular photons, on nuclei. After an outline of the theoretical method used we focus on a discussion of actual observables in photonuclear reactions; we discuss in detail  $2\pi$ - and vector-meson production. We show that the  $2\pi^0$  photoproduction data can be well described by final state interactions of the pions produced whereas the semi-charged  $\pi^0\pi^\pm$  channel exhibits a major discrepancy with theory. For  $\omega$  production on nuclei in the TAPS/CB@ELSA experiment we analyse the  $\pi^0\gamma$  decay channel, and illustrate the strength of the method by simulating experimental acceptance problems. Completely free of final state interactions is dilepton production in the few GeV range. We show that the sensitivity of this decay channel to changes of hadronic properties in medium in photonuclear reactions on nuclei is as large as in ultrarelativistic heavy ion collisions and make predictions for the on-going G7 experiment at JLAB. Finally we discuss that hadron production in nuclei at 10 – 20 GeV photon energies can give important information on the hadronization process, and in particular on the time-scales involved. We show here detailed calculations for the low-energy (12 GeV) run at HERMES and predictions for planned experiments at JLAB.

## 1 Introduction

Studies of in-medium properties of hadrons are driven by a number of - partly connected - motivations. First, there is the expectation that changes of hadronic properties in medium can be precursor phenomena to changes in the phase structure of nuclear matter. Here the transition to the chirally symmetric phase, that exhibits manifestly the symmetries of the underlying theory of strong interactions, i.e. QCD, is of particular interest. Present day's ultrarelativistic heavy-ion collisions explore this phase boundary in the limit of high temperatures ( $T \approx 170$  MeV) and low densities. The other limit (low temperatures and high densities) is harder to reach, although the older AGS heavy-ion experiments and the planned CBM experiment at the new FAIR facility [1] may yield insight into this area. However, even in these experiments the temperatures reached are still sizeable ( $T \approx 120$  MeV). At very low temperatures the only feasible method seems to be the exploration of the hadronic structure inside ordinary nuclei. Here the temperature is  $T = 0$  and the density at most equals the equilibrium density of nuclear matter,  $\rho_0$ . It is thus of great interest to explore if such low densities can already give precursor signals for chiral symmetry restoration. The second motivation for the study of hadronic in-medium properties is provided by our interest in understanding the structure of large dense systems, such as the interior of stars. This structure obviously depends on the composition of stellar matter and its interactions.

In [2] we have discussed the relevant questions and theoretical studies of in-medium properties in some detail. Such calculations necessarily rely on a number of simplifying assumptions, foremost being that of an infinite medium at rest in which the hadron under study is embedded. In actual experiments these hadrons are observed through their decay products and these have to travel through the surrounding nuclear matter to the detectors. Except for the case of electromagnetic signals (photons, dileptons) this is connected with often sizeable final state interactions (FSI) that have to be treated as realistic as possible. For a long period the Glauber approximation which allows only for absorptive processes along a straight-line path has been the method of choice in theories of photonuclear reactions on nuclei. This may be sufficient if one is only interested in total yields. However, it is clearly insufficient when one aims at, for example, reconstructing the spectral function of a hadron inside matter through its decay products. Rescattering and sidefeeding through coupled channel effects can affect the final result so that a realistic description of such effects is absolutely mandatory [3].

In the present paper we present the method used for the full event simulation in some more details while being quite short on the theoretical calculations of in-medium properties. For the latter we refer to [2].

That hadrons can change their properties and couplings in the nuclear medium has been well known since the days of the Delta-hole model that dealt with the changes of the properties of the pion and Delta-resonance inside nuclei [4]. Due to the predominant  $p$ -wave interaction of pions with nucleons one observes a lowering of the pion branch for small, but finite pion momenta, which increases with the nucleon-density. More recently, experiments at the FRS at GSI have shown that also the pion rest mass in medium differs from its value in vacuum [5].

In addition, vector mesons have found an increasing interest over the last few years. These mesons are the first excitations of the QCD vacuum that are not protected by chiral symmetry, as the pions as Goldstone bosons are, and should therefore be more directly related to the chiral condensates. Indeed, the original work by Hatsuda and Lee [6] based on QCD sum rules predicted a significant lowering of the vector meson masses with increasing density, the effect being as large as 30% already at nuclear matter equilibrium density. As discussed in more detail in [2] and in particular in [7, 8] this original prediction strongly depended on simplifying assumptions for the spectral function of the particles involved. When more realistic spectral shapes are used the QCD sum rule gives only certain restrictions on mass and width of the particles involved, but does not fix the latter; for that hadronic models are needed. In particular, for the  $\rho$  meson it turned out that the broadening is more dominant than a mass-shift [9]. This scenario is in line with observations by the CERES experiment [10] that has found a considerable excess of dileptons in an invariant mass range from  $\approx 300$  MeV to  $\approx 700$  MeV as compared to expectations based on the assumption of freely radiating mesons. This result has found an explanation in terms of a shift of the  $\rho$  meson spectral function down to lower masses, as expected from theory (see, e.g., [9, 11, 12, 13]). However, while quite different model calculations tend to explain the data, though often with some model assumptions [14, 15, 16, 17, 18] their theoretical input is sufficiently different as to make the inverse conclusion that the data prove one or another of these scenarios impossible. The more recent experimental results on a change of the rho-meson properties in-medium obtained in an ultrarelativistic  $Au + Au$  collision by the STAR collaboration at RHIC [19] show a downward shift of the  $\rho$ -meson pole mass by about 70 MeV. Since also the  $p + p$  data obtained in the same experiment show a similar, though slightly less pronounced (-40 MeV), shift of the  $\rho$ -meson mass, phase-space distortions of the  $\rho$ -meson spectral shape may be at least partly responsible for the observed mass shift. In the heavy-ion experiment then a number of additional effects, mainly by dynamical interactions with surrounding matter, may contribute, but are hard to separate from the more mundane phase space effects.

One of the authors has, therefore, already some years ago proposed to look for the theoretically predicted changes of vector meson properties inside the nuclear medium in reactions on normal nuclei with more microscopic probes [20, 21, 22]. Of course, the average nuclear density felt by the vector

mesons in such experiments lies much below the equilibrium density of nuclear matter,  $\rho_0$ , so that naively any density-dependent effects are expected to be much smaller than in heavy-ion reactions.

On the other hand, there is a big advantage to these experiments: they proceed with the spectator matter being close to its equilibrium state. This is essential because all theoretical predictions of in-medium properties of hadrons are based on a model in which the hadron (vector meson) under investigation is embedded in nuclear matter in equilibrium and with infinite extension. However, a relativistic heavy-ion reaction proceeds – at least initially – far from equilibrium. Even if equilibrium is reached in a heavy-ion collision this state changes by cooling through expansion and particle emission and any observed signal is built up by integrating over the emissions from all these different stages of the reaction.

Another in-medium effect arises when particles are produced by high-energy projectiles inside a nuclear medium. A major experimental effort at RHIC experiments has gone into the observation of jets in ultra-relativistic heavy-ion collisions and the determination of their interaction with the surrounding quark or hadronic matter [23]. A complementary process is given by the latest HERMES results at HERA for high-energy electroproduction of hadrons off nuclei [24]. Again, the advantage of the latter experiment is that the nuclear matter with which the interactions happen is at rest and in equilibrium.

In this lecture note we summarize results that we have obtained in studies of observable consequences of in-medium changes of hadronic spectral functions as well as hadron formation in reactions of elementary probes with nuclei. We demonstrate that the expected in-medium sensitivity in such reactions is as high as that in relativistic heavy-ion collisions and that in particular photonuclear reactions present an independent, cleaner testing ground for assumptions made in analyzing heavy-ion reactions.

## 2 Theory

### 2.1 QCD Sum Rules and Hadronic Models

A review of the underlying theory can be found in [2]. Here we would just like to mention that the connection between chiral condensates on one hand and hadronic observables on the other cannot simply be inferred from looking at the dependence of the condensate on density and temperature. Instead, the connection is much more indirect; only an integral over the spectral function can be linked via the QCD sum rule to the condensate behavior in medium. In an abbreviated form this connection is given by

$$R^{\text{OPE}}(Q^2) = \frac{\tilde{c}_1}{Q^2} + \tilde{c}_2 - \frac{Q^2}{\pi} \int_0^\infty ds \frac{\text{Im}R^{\text{HAD}}(s)}{(s + Q^2)s} \quad (1)$$

with  $Q^2 := -q^2 \gg 0$  and some subtraction constants  $\tilde{c}_i$ . Here  $R^{\text{OPE}}$  represents a Wilson's operator expansion of the current-current correlator in terms of quark and gluon degrees of freedom in the space-like region. It is an expansion in terms of powers of  $1/Q^2$  and contains the condensates as expansion parameters. On the other hand,  $R^{\text{HAD}}(s)$  in (1) is the same object for time-like momenta, represented by a parametrization in terms of hadronic variables. The dispersion integral connects time- and space-like momenta. Eq. (1) connects the hadronic with the quark world. It allows to determine parameters in a hadronic parametrization of  $R^{\text{HAD}}(s)$  by comparing the lhs of this equation with its rhs. Invoking vector meson dominance it is easy to see that for vector mesons  $\text{Im}R^{\text{HAD}}(s)$  in (1) is just the spectral function of the meson under study.

The operator product expansion of  $R^{\text{OPE}}$  on the lhs involves quark- and gluon condensates [7, 8]; of these only the two-quark condensates are reasonably well known, whereas our knowledge about already the four-quark condensates is rather sketchy.

Using the measured, known vacuum spectral function for  $R^{\text{HAD}}$  allows one to obtain information about these condensates appearing on the lhs of (1). On the other hand, modelling the density-

dependence of the condensates yields information on the change of the hadronic spectral function when the hadron is embedded in nuclear matter. Since the spectral function appears under an integral the information obtained is not direct. Therefore, as Leupold et al. have shown [7, 8], the QCDSR provides important constraints for the hadronic spectral functions in medium, but it does not fix them. Recently Kaempfer et al have turned this argument around by pointing out that measuring an in-medium spectral function of the  $\omega$  meson could help to determine the density dependence of the higher-order condensates [25].

Thus models are needed for the hadronic interactions. The quantitatively reliable ones can at present be based only on 'classical' hadrons and their interactions. Indeed, in lowest order in the density the mass and width of an interacting hadron in nuclear matter at zero temperature and vector density  $\rho_v$  are given by (for a meson, for example)

$$\begin{aligned} m^{*2} &= m^2 - 4\pi \mathcal{R}e f_{mN}(q_0, \theta = 0) \rho_v \\ m^* \Gamma^* &= m \Gamma^0 - 4\pi \mathcal{I}m f_{mN}(q_0, \theta = 0) \rho_v . \end{aligned} \quad (2)$$

Here  $f_{mN}(q_0, \theta = 0)$  is the forward scattering amplitude for a meson with energy  $q_0$  on a nucleon. The width  $\Gamma^0$  denotes the free decay width of the particle. For the imaginary part this is nothing other than the classical relation  $\Gamma^* - \Gamma^0 = v\sigma\rho_v$  for the collision width, where  $\sigma$  is the total cross section. This can easily be seen by using the optical theorem.

Unfortunately it is not a-priori known up to which densities the low-density expansion (2) is useful. Post et al. [9] have recently investigated this question in a coupled-channel calculation of selfenergies. Their analysis comprises pions,  $\eta$ -mesons and  $\rho$ -mesons as well as all baryon resonances with a sizeable coupling to any of these mesons. The authors of [9] find that already for densities less than  $0.5\rho_0$  the linear scaling of the selfenergies inherent in (2) is badly violated for the  $\rho$  and the  $\pi$  mesons, whereas it is a reasonable approximation for the  $\eta$  meson. Reasons for this deviation from linearity are Fermi-motion, Pauli-blocking, selfconsistency and short-range correlations. For different mesons different sources of the discrepancy prevail: for the  $\rho$  and  $\eta$  mesons the iterations act against the low-density theorem by inducing a strong broadening for the  $D_{13}(1520)$  and a slightly repulsive mass shift for the  $S_{11}(1535)$  nucleon resonances to which the  $\rho$  and the  $\eta$  meson, respectively, couple. The investigation of in-medium properties of mesons, for example, thus involves at the same time the study of in-medium properties of nucleon resonances and is thus a coupled-channel problem.

## 2.2 Coupled Channel Treatment of Incoherent Particle Production

Very high nuclear densities ( $2 - 8\rho_0$ ) and temperatures  $T$  up to or even higher than  $\approx 170$  MeV can be reached with present day's accelerators in heavy-ion collisions. Thus, any density-dependent effect gets magnified in such collisions. However, the observed signal always represents a time-integral over various quite different stages of the collision – non-equilibrium and equilibrium, the latter at various densities and temperatures. The observables thus have to be modelled in a dynamic theory. In contrast, the theoretical input is always calculated under the simplifying assumption of a hadron in stationary nuclear matter in equilibrium and at fixed density. The results of such calculations are then used in dynamical simulations of various degrees of sophistication most of which invoke a quasi-stationary approximation. In order to avoid these intrinsic difficulties we have looked for possible effects in reactions that proceed closer to equilibrium, i.e. reactions of elementary probes such as protons, pions, and photons on nuclei. The densities probed in such reactions are always  $\leq \rho_0$ , with most of the nucleons actually being at about  $0.5\rho_0$ . On the other hand, the target is stationary and the reaction proceeds much closer to (cold) equilibrium than in a relativistic heavy-ion collision. If any observable effects of in-medium changes of hadronic properties survive, even though the densities probed are always  $\leq \rho_0$ , then the study of hadronic in-medium properties in reactions with elementary probes on nuclei provides an essential baseline for in-medium effects in hot nuclear matter probed in ultra-relativistic heavy-ion collisions.

With the aim of exploring this possibility we have over the last few years undertaken a number of calculations for proton- [26], pion- [27, 28] and photon- [29] induced reactions. All of them have one feature in common: they treat the final state incoherently in a coupled channel transport calculation that allows for elastic and inelastic scattering of, particle production by and absorption of the produced hadrons. A new feature of these calculations is that hadrons with their correct spectral functions can actually be produced and transported consistently. This is quite an advantage over earlier treatments [30, 31] in which the mesons were always produced and transported with their pole mass and their spectral function was later on folded in only for their decay. The method is summarized in the following section, more details can be found in [29].

We separate the photonuclear reaction into three steps. First, we determine the amount of shadowing for the incoming photon; this obviously depends on its momentum transfer  $Q^2$ . Second, the primary particle is produced and third, the produced particles are propagated through the nuclear medium until they leave the nucleus.

**Shadowing.** Photonuclear reactions show shadowing in the entrance channel, for real photons from an energy of about 1 GeV on upwards [32]. This shadowing is due to a coherent superposition of bare photon and vector meson components in the incoming photon and is handled here by means of a Glauber multiple scattering model [3]. In this way we obtain for each value of virtuality  $Q^2$  and energy  $\nu$  of the photon a spatial distribution for the probability that the incoming photon reaches a given point; for details see [3, 33, 34]. Fig. 2.2 gives an example of the spatial distribution for a kinematical situation which is close to that of the HERMES experiment. The function shown in Fig. 2.2 gives the

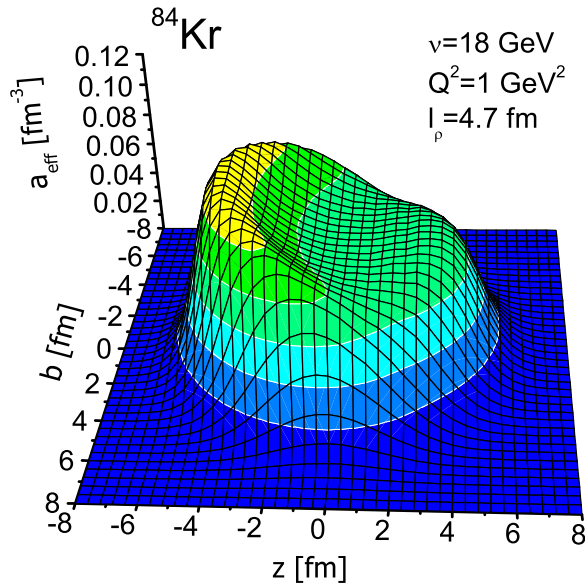


Figure 1: Profile function for shadowing. Shown is the probability distribution for the interaction of an incoming photon (from left) with given virtuality and energy with nucleons in a  $^{208}\text{Pb}$  nucleus (from [3]).

probability distribution that the incoming photon hits the nucleon at that point.

**Initial Production.** The initial particle production is handled differently depending on the invariant mass  $W = \sqrt{s}$  of the excited state of the nucleon. If  $W < 2$  GeV, we invoke a nucleon resonance model that has been adjusted to nuclear data on resonance-driven particle production [29]. If  $W > 2$  GeV the particle yield is calculated with standard codes developed for high energy nuclear reactions, i.e. FRITIOF or PYTHIA; details are given in [35]. We have made efforts to ensure a smooth transition of cross sections in the transition from resonance physics to DIS.

**Final State Interactions.** The final state is described by a semiclassical coupled channel transport model that had originally been developed for the description of heavy-ion collisions and has since then been applied to various more elementary reactions on nuclei with protons, pions and photons in the entrance channel.

In this method the spectral phase space distributions of all particles involved are propagated in time, from the initial first contact of the photon with the nucleus all the way to the final hadrons leaving the nuclear volume on their way to the detector. The spectral phase space distributions  $F_h(\vec{x}, \vec{p}, \mu, t)$  give at each moment of time and for each particle class  $h$  the probability to find a particle of that class with a (possibly off-shell) mass  $\mu$  and momentum  $\vec{p}$  at position  $\vec{x}$ . Its time-development is determined by the BUU equation

$$\left(\frac{\partial}{\partial t} + \frac{\partial H_h}{\partial \vec{p}} \frac{\partial}{\partial \vec{r}} - \frac{\partial H_h}{\partial \vec{r}} \frac{\partial}{\partial \vec{p}}\right) F_h = G_h \mathcal{A}_h - L_h F_h. \quad (3)$$

Here  $H_h$  gives the energy of the hadron  $h$  that is being transported; it contains the mass, the selfenergy (mean field) of the particle and a term that drives an off-shell particle back to its mass shell. The terms on the lhs of (3) are the so-called *drift terms* since they describe the independent transport of each hadron class  $h$ . The terms on the rhs of (3) are the *collision terms*; they describe both elastic and inelastic collisions between the hadrons. Here the term *inelastic collisions* includes those collisions that either lead to particle production or particle absorption. The former is described by the *gain term*  $G_h \mathcal{A}_h$  on the rhs in (3), the latter process (absorption) by the *loss term*  $L_h F_h$ . Note that the gain term is proportional to the spectral function  $\mathcal{A}$  of the particle being produced, thus allowing for production of off-shell particles. On the contrary, the loss term is proportional to the spectral phase space distribution itself: the more particles there are the more can be absorbed. The terms  $G_h$  and  $L_h$  on the rhs give the actual strength of the gain and loss terms, respectively. They have the form of Born-approximation collision integrals and take the Pauli-principle into account. The free collision rates themselves are taken from experiment or are calculated [29].

Eq. (3) contains a selfconsistency problem. The collision rates embedded in  $G$  and  $L$  determine the collisional broadening of the particles involved and thus their spectral function  $\mathcal{A}$ . The widths of the particles, resonances or mesons, thus evolve in time away from their vacuum values. In addition, broad particles can be produced off their peak mass and then propagated. The extra 'potential' in  $H$  already mentioned ensures that all particles are being driven back to their mass-shell when they leave the nucleus. The actual method used is described in [29]. It is based on an analysis of the Kadanoff-Baym equation that has led to practical schemes for the propagation of off-shell particles [36, 37]. The possibility to transport off-shell particles represents a major breakthrough in this field. For further details of the model see Ref. [29] and [35] and references therein.

### 3 Particle Production on Nuclei – Observables

#### 4 $\eta$ Production

We first look at the prospects of using reactions with hadronic final states and discuss the photo-production of  $\eta$ -mesons on nuclei as a first example. These mesons are unique in that they are sensitive

to one dominating resonance the  $S_{11}(1535)$  so that one may hope to learn something about the properties of this resonance inside nuclei. Experiments for this reaction were performed both by the TAPS collaboration [38, 39] and at KEK [40].

Estimates of the collisional broadening of the  $S_{11}(1535)$  resonance have given a collision width of about 35 MeV at  $\rho_0$  [41]. The more recent, and more refined, selfconsistent calculations of [9] give a very similar value for this resonance. In addition, a dispersive calculation of the real part of the selfenergy for the resonance at rest gives only an insignificant shift of the resonance position. Thus any momentum-dependence of the selfenergy as observed in photon-nucleus data can directly be attributed to binding energy effects [42]. The results obtained in [42] indicate that the momentum dependence of the  $N^*(1535)$  potential has to be very similar to that of the nucleons.

The particular advantage of our coupled-channels approach can be seen in Fig. 2 which shows results both for photon- and electroproduction of  $\eta$ 's on nuclei; for the latter process so far no data are available. The calculations give the interesting result that for photo-production a secondary reaction

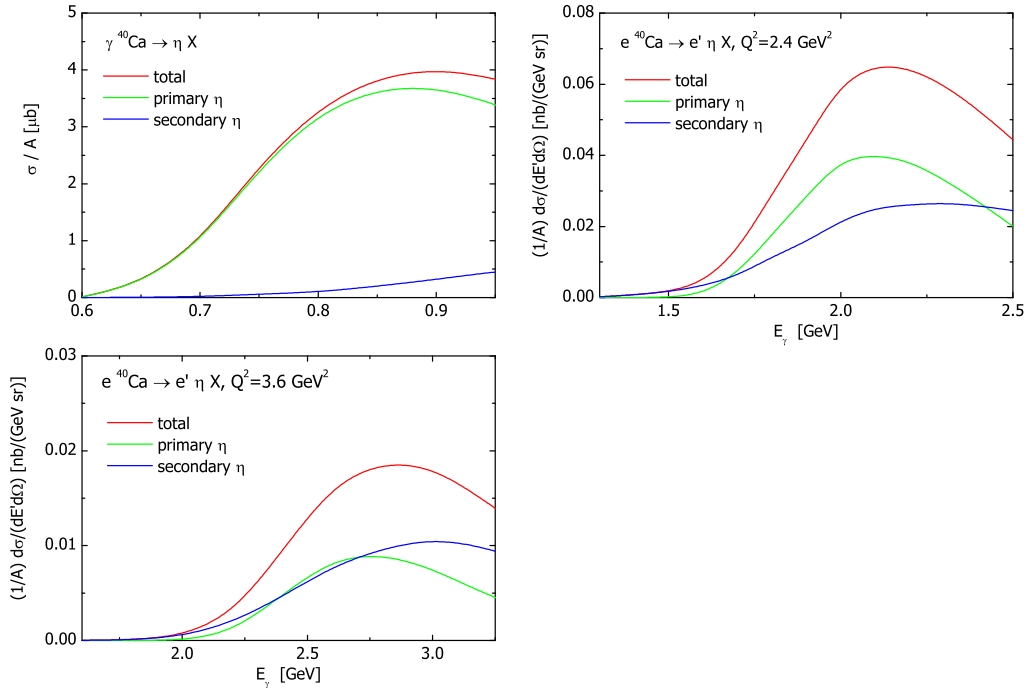


Figure 2: Eta-electroproduction cross sections on  $^{40}\text{Ca}$  for three values of  $Q^2$  given in the figures. The uppermost curve in all three figures gives the total observed yield, the next curve from top gives the contribution of the direct  $\eta$  production channel and the lowest curve shows the contribution of the secondary process  $\pi N \rightarrow \eta N$ . For the highest value of  $Q^2 = 3.6 \text{ GeV}^2$  the primary and secondary production channels nearly coincide (from [43]).

channel becomes important at high energies and virtualities. In this channel first a pion is produced which travels through the nucleus and through  $\pi N \rightarrow N^*(1535) \rightarrow N\eta$  produces the  $\eta$  that is finally observed in experiment. This channel becomes even dominant for high  $Q^2$  electroproduction. In both cases the reason for the observed growing of the importance of secondary production channels lies in the higher momentum transferred to the initial pion [43].

## 4.1 $2\pi$ Production

If chiral symmetry is restored, the masses of the scalar isoscalar  $\sigma$  meson and that of the scalar isovector pion should become degenerate. This implies that the spectral function of the  $\sigma$  should become softer and narrower with its strength moving down to the  $2\pi$  threshold. This leads to a threshold enhancement in the  $\pi\pi$  invariant mass spectrum due to suppression of the phase-space for the  $\sigma \rightarrow \pi\pi$  decay.

A first measurement of the two pion invariant mass spectrum has been obtained by the CHAOS collaboration in pion induced reactions on nuclei [44]. The authors of [44] claimed to indeed have seen an accumulation of spectral strength near the  $2\pi$  threshold for heavy target nuclei in the  $\pi^+\pi^-$  mass distribution. According to the arguments presented in the introduction, photon induced reactions in nuclei are much better suited to investigate double pion production at finite baryon densities. A recent experiment with the TAPS spectrometer at the tagged-photon facility MAMI-B in Mainz indeed shows an even more pronounced accumulation of spectral strength of the two pion mass spectrum for low invariant masses with increasing target mass corresponding to increasing average densities probed [45]. This accumulation has been observed for the  $\pi^0\pi^0$  but not for the  $\pi^\pm\pi^0$  final state.

These results have been explained by a model developed by Roca et al. [46]. In this model the  $\sigma$  meson is generated dynamically as a resonance in the  $\pi\pi$  scattering amplitude. By dressing the pion propagators in the medium by particle-hole loops, they found the observed downward shift of the  $\pi\pi$  mass spectrum to be consistent with a dropping of the  $\sigma$ -pole in the  $\pi\pi$  scattering amplitude, i. e. a lowering of the  $\sigma$  meson mass.

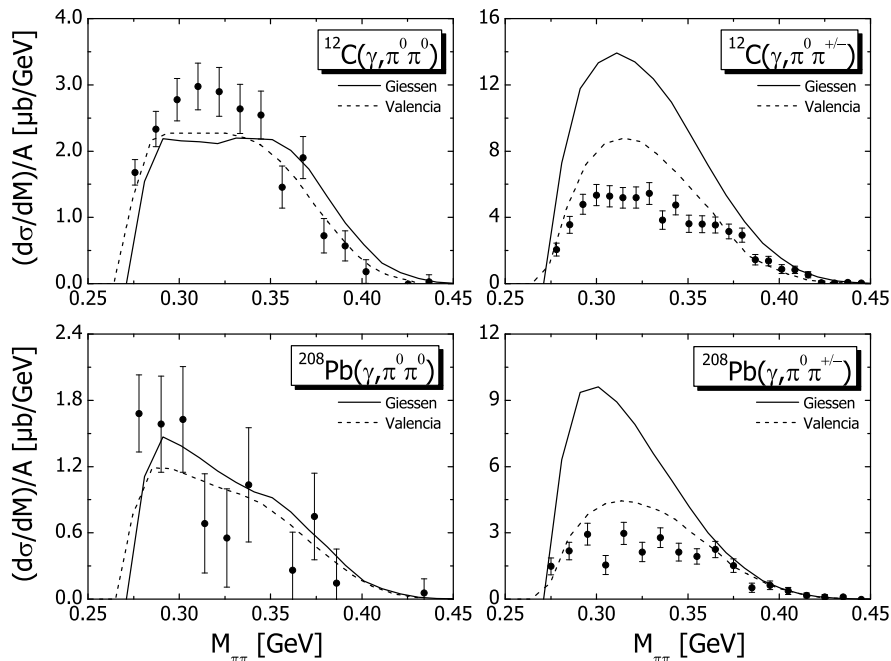


Figure 3: Two pion invariant mass distributions for the  $\pi^0\pi^0$  (left) and  $\pi^0\pi^\pm$  (right) photo-production on  $^{12}\text{C}$  and  $^{208}\text{Pb}$  (from [47]). The solid lines represent our results whereas the dashed lines labelled “Valencia” depict the results of ref. [46].

In analyzing the TAPS data it is absolutely essential to simulate the final state interactions of the outgoing pions, correlated or not, in an as realistic way as possible. We have, therefore, taken the conservative approach of analyzing this reaction without any changes of the  $\sigma$  spectral function in the outgoing channel. The result of this study [47] is shown in Fig. 3.



Fig. 3 shows on its left side that the observed downward shift of the  $2\pi^0$  mass spectrum can be well reproduced by final state interactions on the independent pions without any in-medium modification of the  $\pi\pi$  interaction. This shift can be attributed to a slowing down of the pions due to quasi elastic collisions with the nucleons in the surrounding nuclear medium. Also shown is the result of the calculations of Roca et al. [46]. Both calculations obviously agree with each other so that the final observables are fairly independent of any  $\pi\pi$  correlations.

On the right side of Fig. 3 the results for the semi-charged  $\pi^0\pi^\pm$  channel are shown. Here our theoretical result (solid line) overestimates the data by up to a factor of 3. The result obtained in Ref. [46] also lies too high, but by a lesser amount; this has been explained in [47] by the neglect of charge-transfer channels in the calculations of Roca et al. [46]. The observed discrepancy with experiment for this channel is astounding since the method used normally describes data within a much narrower error band. Thus understanding this discrepancy is absolutely essential before a shift or non-shift in the mass distribution for this channel can be ascertained.

## 4.2 $\omega$ Production

Many of the early studies of hadronic properties in medium concentrated on the  $\rho$ -meson [11, 49], partly because of its possible significance for an interpretation of the CERES experiment. It is clear by now, however, that the dominant effect on the in-medium properties of the  $\rho$ -meson is collisional broadening that overshadows any possible mass shifts [9] and is thus experimentally hard to observe. The emphasis has, therefore, shifted to the  $\omega$  meson. An experiment measuring the  $A(\gamma, \omega \rightarrow \pi^0\gamma')X$  reaction is presently being analyzed by the TAPS/Crystal Barrel collaborations at ELSA [48]. The varying theoretical predictions for the  $\omega$  mass (640-765 MeV) [49] and width (up to 50 MeV) [27, 50] in nuclear matter at rest encourage the use of such an exclusive probe to learn about the  $\omega$  spectral distribution in nuclei.

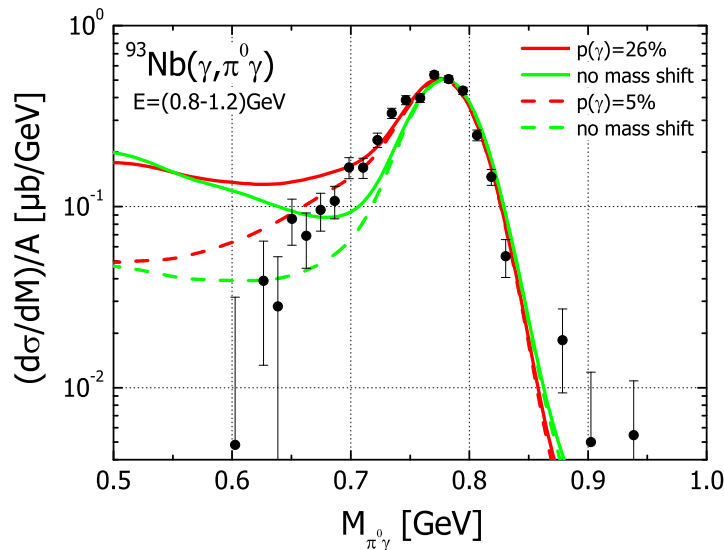


Figure 4: Mass differential cross section for  $\pi^0\gamma$  photoproduction off  $^{93}\text{Nb}$ . Shown are results both with and without a mass-shift as explained in [51]. The quantity  $p$  gives the escape probability for one of the four photons in the  $2\pi^0$  channel. The two solid curves give results of calculations with  $p = 26\%$  with and without mass-shift, the two dashed curves give the same for  $p = 5\%$

Simulations have been performed at 1.2 GeV and 2.5 GeV photon energy, which cover the accessible

energies of the TAPS/Crystal Barrel experiment. After reducing the combinatorial and rescattering background by applying kinematic cuts on the outgoing particles, we have obtained rather clear observable signals for an assumed dropping of the  $\omega$  mass inside nuclei [51]. Therefore, in this case it should be possible to disentangle the collisional broadening from a dropping mass, which may be related to a change of the chiral condensate at finite nuclear density [52].

Our calculations represent complete event simulations. It is, therefore, possible to take experimental acceptance effects into account. An example is shown in Fig. 4 which shows the effects of a possible misidentification of the  $\omega$  meson. This misidentification can come about through the  $2\pi^0 \rightarrow 4\gamma$  channel if one of the four photons escapes detection and the remaining three photons are identified as stemming from the  $\pi^0\gamma \rightarrow 3\gamma$  decay channel of the  $\omega$ -meson.

Fig. 4 shows a good agreement between the preliminary data of the TAPS/CB@ELSA collaboration [53] for a photon escape probability of 5 % and a mass shift  $m_\omega = m_\omega^0 - 0.18 \rho/\rho_0$ . In [51, 2] we have also discussed the momentum-dependence of the  $\omega$ -selfenergy in medium and have pointed out that this could be accessible through measurements which gate on different three-momenta of the  $\omega$  decay products.

### 4.3 Dilepton Production

Dileptons, i.e. electron-positron pairs, in the outgoing channel are an ideal probe for in-medium properties of hadrons since they experience no strong final state interaction. A first experiment to look for these dileptons in heavy-ion reactions was the DLS experiment at the BEVALAC in Berkeley [54]. Later on, and in a higher energy regime, the CERES experiment has received a lot of attention for its observation of an excess of dileptons with invariant masses below those of the lightest vector mesons [10]. Explanations of this excess have focused on a change of in-medium properties of these vector mesons in dense nuclear matter (see e.g. [14, 15]). The radiating sources can be nicely seen in Fig. 5 that shows the dilepton spectrum obtained in a low-energy run at 40 AGeV together with the elementary sources of dilepton radiation.

The figure exhibits clearly the rather strong contributions of the vector mesons – both direct and through their Dalitz decay – at invariant masses above about 500 MeV. The strong amplification of the dilepton rate at small invariant masses  $M$  caused by the photon propagator, which contributes  $\sim 1/M^4$  to the cross section, leads to a strong sensitivity to changes of the spectral function at small masses. Therefore, the excess observed in the CERES experiment can be explained by such changes as has been shown by various authors (see e.g. [30] for a review of such calculations).

In view of the uncertainties in interpreting these results discussed earlier we have studied the dilepton photo-production in reactions on nuclear targets. Looking for in-medium changes in such a reaction is not *a priori* hopeless: Even in relativistic heavy-ion reactions only about 1/2 of all dileptons come from densities larger than  $2\rho_0$  [30]. In these reactions the pion-density gets quite large in the late stages of the collision. Correspondingly many  $\rho$  mesons are formed (through  $\pi + \pi \rightarrow \rho$ ) late in the collision, where the baryonic matter expands and its density becomes low again.

6. In [29] we have analyzed the photoproduction of dileptons on nuclei in great detail. After removing the Bethe-Heitler contribution the dilepton mass spectrum in a 2 GeV photon-induced reaction looks very similar to that obtained in an ultrarelativistic heavy-ion collision (Fig. 5). The radiation sources are all the same in both otherwise quite different reactions. The photon-induced reaction can thus be used as a baseline experiment that allows one to check crucial input into the simulations of more complicated heavy-ion collision.

A typical result of such a calculation for the dilepton yield – after removing the Bethe-Heitler component – is given in Fig. 6. The lower part of Fig. 6 shows that we can expect observable effect of possible in-medium changes of the vector meson spectral functions in medium on the low-mass side of the  $\omega$  peak. In [29] we have shown that these effects can be drastically enhanced if proper kinematic

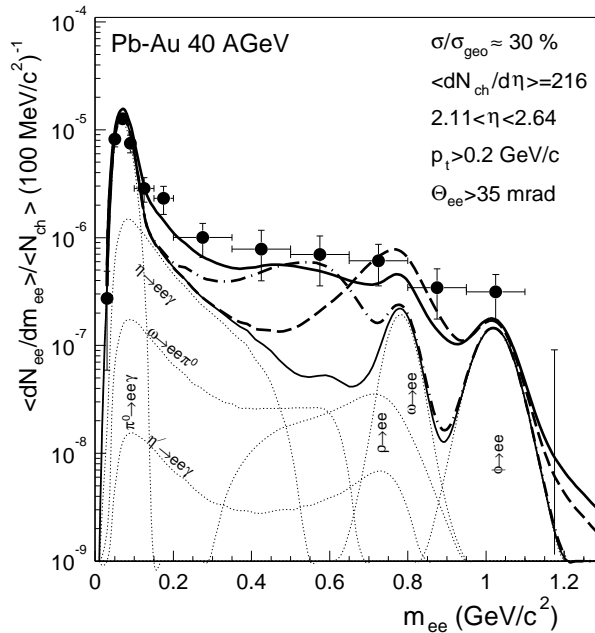


Figure 5: Invariant dilepton mass spectrum obtained with the CERES experiment in Pb + Au collisions at 40 AGeV (from [10]). The thin curves give the contributions of individual hadronic sources to the total dilepton yield, the fat solid (modified spectral function) and the dash-dotted (dropping mass only) curves give the results of calculations [16] employing an in-medium modified spectral function of the vector mesons.

cuts are introduced that tend to enhance the in-medium decay of the vector mesons. There it was shown that in the heavy nucleus *Pb* the  $\omega$ -peak completely disappears from the spectrum if in-medium changes of width and mass are taken into account. The sensitivity of such reactions is thus as large as that observed in ultrarelativistic heavy-ion reactions.

An experimental verification of this prediction would be a major step forward in our understanding of in-medium changes. The ongoing G7 experiment at JLAB is presently analyzing such data [55]. This experiment can also yield important information on the time-like electromagnetic formfactor of the proton and its resonances [56] on which little or nothing is known.

## 5 Hadron Formation

Hadron production in reactions of high energy photons and leptons on complex nuclei give us insight into the physics of hadron formation. The products of a (virtual) photon-nucleon interaction need a finite time to evolve to physical hadrons. Since the hadronization process itself is of nonperturbative nature it is not well understood. The formation time of a hadron may be estimated by the time that its constituents need to travel a hadronic radius and, hence, should be of the order of 0.5–0.8 fm/c in the rest frame of the hadron. Due to time dilatation the formation lengths in the lab frame can become quite large. For high energy particles they can easily exceed the nuclear radius. Therefore, a heavy nucleus can serve as a kind of 'microdetector' which is situated directly behind the interaction vertex and which probes the interaction of the reaction products prior to hadronization. Hence, high energy (virtual) photonuclear reactions provide us with essential information on the time scales of hadron formation as well as the nature of prehadronic final state interactions. Obviously, the latter is closely

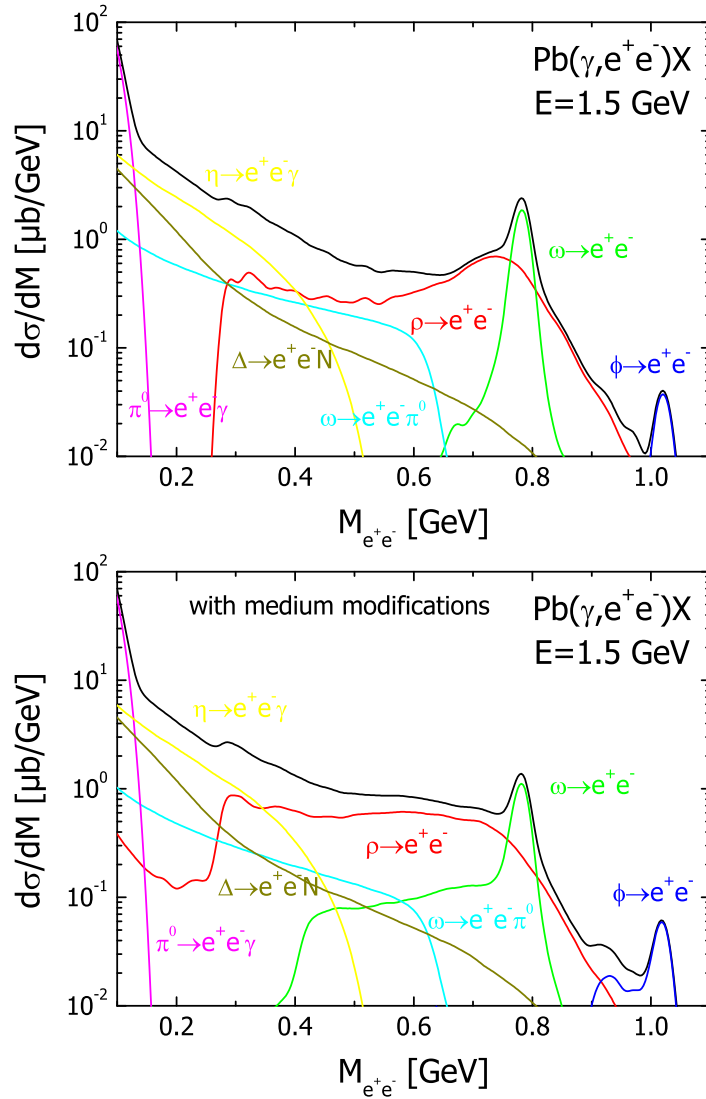


Figure 6: Hadronic contributions to dilepton invariant mass spectra for  $\gamma + {}^{208}\text{Pb}$  at 1.5 GeV photon energy). Indicated are the individual contributions to the total yield; compare with Fig. 5.

related to color transparency.

The HERMES collaboration [24] has studied hadron production in deep inelastic lepton scattering off various nuclei. Depending on the lepton beam energy used at HERA the photon-energies are of the order of  $\nu = 2\text{--}20$  GeV, with rather moderate  $Q^2 \approx 1\text{--}2$  GeV<sup>2</sup>. A similar experiment is currently performed by the CLAS collaboration at Jefferson Lab [57] using a 5 GeV electron beam. After the planned energy upgrade they will reach photon energies of the order of  $\nu = 2\text{--}9$  GeV and similar virtualities as in the HERMES experiment.

The observed multiplicity spectra have led to a numerous different interpretations. They reach from a purely partonic energy loss through induced gluon radiation of the struck quark propagating through the nucleus [58] to a possible rescaling of the quark fragmentation function at finite nuclear density combined with hadron absorption in the nuclear environment [59]. Note that the detailed understanding of hadron attenuation in cold nuclear matter can serve as a useful basis for the interpretation of jet quenching observed in ultra-relativistic heavy ion collisions at RHIC.

In our approach [35, 60] we assume that the virtual photon interacts with the bound nucleon either

directly or via one of its hadronic fluctuations. The hadronic components of the photon are thereby shadowed according to the method described in Sec. 2.2 which allows for a clean-cut separation of the coherent initial state interactions of the photon and the incoherent final state interactions of the reaction products. The photon-nucleon interaction leads to the excitation of one or more strings which fragment into color-neutral prehadrons due to the creation of quark-antiquark pairs from the vacuum. As discussed by Kopeliovich et al. [61] the production time of these prehadrons is very short. For simplicity we set the production time to zero in our numerical realization. These prehadrons are then propagated using our coupled-channel transport theory.

After a formation time which we assume to be a constant  $\tau_f$  in the restframe of the hadron the hadronic wave function has built up and the reaction products behave like usual hadrons. The prehadronic cross sections  $\sigma^*$  during the formation time are determined by a simple constituent quark model

$$\begin{aligned}\sigma_{\text{prebaryon}}^* &= \frac{n_{\text{org}}}{3} \sigma_{\text{baryon}}, \\ \sigma_{\text{premeson}}^* &= \frac{n_{\text{org}}}{2} \sigma_{\text{meson}},\end{aligned}\quad (4)$$

where  $n_{\text{org}}$  denotes the number of (anti-)quarks in the prehadron stemming from the beam or target. As a consequence the prehadrons that solely contain (anti-)quarks produced from the vacuum in the string fragmentation do not interact during  $\tau_f$ . Using this recipe the total effective cross section of the final state rises like in the approach of Ref. [62] each time when a new hadron has formed.

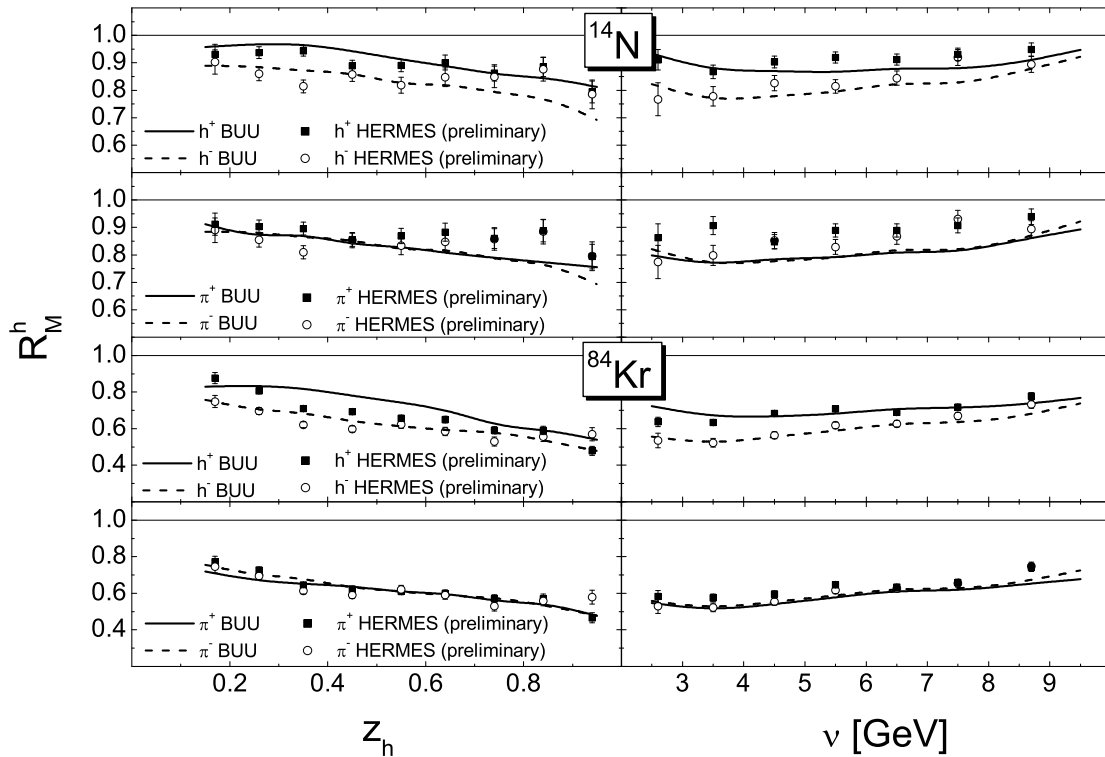


Figure 7: Calculated multiplicity ratio of positively and negatively charged hadrons and pions for a  $^{14}\text{N}$  and  $^{84}\text{Kr}$  target when using a 12 GeV positron beam at HERMES. For the calculation we use the formation time  $\tau_f = 0.5$  fm/c and the constituent-quark concept (4) for the prehadronic cross sections. The data are taken from Ref. [63].

Due to our coupled channel-treatment of the final state interactions the (pre)hadrons might not only be absorbed in the nuclear medium but can produce new particles in an interaction, thereby shifting strength from the high to the low energy part of the hadron spectrum. In addition our event-by-event

simulation allows us to account for all sorts of kinematic cuts and the acceptance of the detector. In Ref. [35] we have demonstrated that our calculations are in excellent agreement with the experimental HERMES data [24] taken on various nuclear targets at beam energy  $E_{\text{beam}} = 27.6$  GeV if one assumes a formation time  $\tau_f = 0.5$  fm/c for all hadron species.

In Fig. 7 we show that our approach is also capable to describe the observed multiplicities of charged hadrons and pions at half the possible beam energy in the HERMES experiment, i.e. at  $E_{\text{beam}} = 12$  GeV. This makes us confident that our model can also be applied for the electron beam energies that will be used at Jefferson Lab.

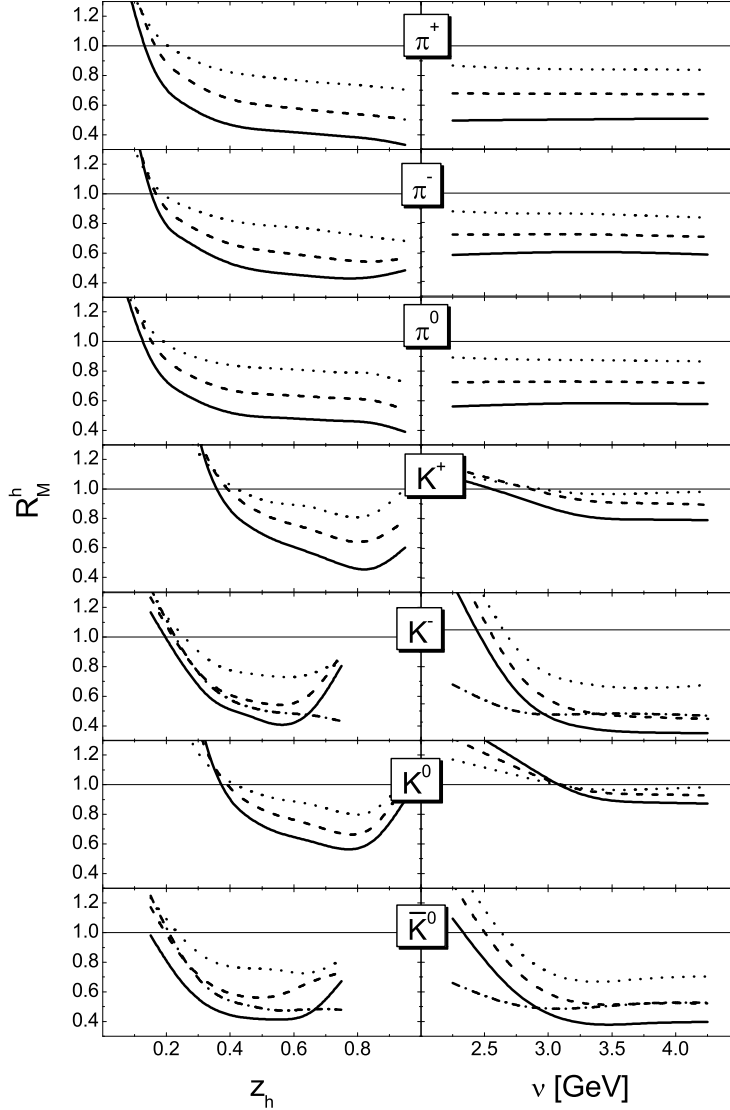


Figure 8: Calculated multiplicity ratio of identified  $\pi^\pm$ ,  $\pi^0$ ,  $K^\pm$ ,  $K^0$  and  $\bar{K}^0$  for  $^{12}\text{C}$  (dotted lines),  $^{56}\text{Fe}$  (dashed lines) and  $^{208}\text{Pb}$  nuclei (solid lines). The simulation has been done for a 5 GeV electron beam and the CLAS detector. The dash-dotted line represents a calculation for  $^{56}\text{Fe}$  without Fermi motion. In all calculations we use the formation time  $\tau_f = 0.5$  fm/c and the constituent-quark concept (4) for the prehadronic cross sections (from [64]).

In Fig. 8 we present our predictions for the multiplicity ratios of identified hadrons at 5 GeV electron beam energy. Besides the considerably lower beam energy used at Jefferson Lab the major difference to the HERMES experiment is the much larger geometrical acceptance of the CLAS detector. The latter leads to an increased detection of low energy secondary particles that are produced in the final state interactions and that lead to a strong increase of the multiplicity ratio at low fractional hadron

energies  $z_h = E_h/\nu$ . In addition, the relatively small average photon energy leads to a visible effect of Fermi motion on the multiplicity ratio of more massive particles. Since the virtual photon cannot produce antikaons without an additional strange meson, e.g.  $\gamma^*N \rightarrow K\bar{K}N$ , the maximum fractional energy  $z_h$  is limited to 0.9 for antikaons. Because of the energy distribution in the three body final state and the finite virtuality of the photon – set by the kinematic cut  $Q^2 > 1 \text{ GeV}^2$  – the maximum fractional energy of antikaons is further reduced. As a result, the  $z_h$  spectra for  $K^-$  and  $\bar{K}^0$  in Fig. 8 do not exceed  $z_h \approx 0.8$ . For the same reason the production of antikaons with  $z_h > 0.2$  is reduced at the lower end of the photon spectrum. The Fermi motion in the nucleus enhances the yield of antikaons in these two extreme kinematic regions as can be seen by comparison with the dash-dotted line in Fig. 8 which represents the result of a calculation for  $^{54}\text{Fe}$  where Fermi motion has been neglected. Certainly, the kaons can be produced in a two body final state (e.g.  $\gamma^*N \rightarrow K\Lambda$ ), however, the accompanying hyperon has a relatively large mass. Therefore, similar, although less pronounced, effects show also up for the kaons. Beside the effects of Fermi motion the multiplicity ratios of kaons and antikaons show the same features as for higher energies.

## 6 Conclusions

In this lecture note we have shown that photonuclear reactions on nuclei can give observable consequences of in-medium changes of hadrons that are as big as those expected in heavy-ion collisions which reach much higher energies, but proceed farther away from equilibrium. Information from photonuclear reactions is important and relevant for an understanding of high density – high temperature phenomena in ultrarelativistic heavy-ion collisions. Special emphasis was put in this article not so much on the theoretical calculations of hadronic in-medium properties under simplified conditions, but more on the final, observable effects of any such properties. We have discussed that for reliable predictions of observables one has to take the final state interactions with all their complications in a coupled channel calculation into account; simple Glauber-type descriptions are not sufficient. We have, for example, shown that in photonuclear reactions in the 1 - 2 GeV range the expected sensitivity of dilepton spectra to changes of the  $\rho$ - and  $\omega$  meson properties in medium is as large as that in ultrarelativistic heavy-ion collisions and that exactly the same sources contribute to the dilepton yield in both experiments. We have also illustrated that the analysis of hadron production spectra in high-energy electroproduction experiments at HERMES gives information about the interaction of forming hadrons with the surrounding hadronic matter. This is important for any analysis that tries to obtain signals for a QGP by analysing high-energy jet formation in ultrarelativistic heavy-ion reactions.

## Acknowledgement

This work has been supported by the Deutsche Forschungsgemeinschaft, the BMBF and GSI Darmstadt.

## References

- [1] <http://www.gsi.de/zukunftsprojekt/index.html>
- [2] T. Falter et al., *Progr. Part. Nucl. Phys.* **53** (2004) 25.
- [3] T. Falter, U. Mosel, *Phys. Rev.* **C66**, 024608 (2002).
- [4] T. Ericson and W. Weise, *Pions and Nuclei*, Clarendon Press, Oxford, 1988.
- [5] H. Geissel et al., *Phys. Rev. Lett.* **88**, 122301 (2002).

- [6] T. Hatsuda, S. H. Lee, *Phys. Rev.* **C46**, 34 (1992).
- [7] S. Leupold, *Phys. Rev.* **C64**, 015202 (2001).
- [8] S. Leupold, U. Mosel, *Phys. Rev.* **C58**, 2939 (1998); S. Leupold et al., *Nucl. Phys.* **A628**, 311 (1998).
- [9] M. Post, S. Leupold and U. Mosel, *Nucl. Phys.* **A741**, 81 (2004).
- [10] J.P. Wessels et al., *Quark Matter 2002 (QM 2002)*, Nantes, France, 18-24 July 2002, *Nucl. Phys.* **A715**, 262 (2003).
- [11] W. Peters et al., *Nucl. Phys.* **A632**, 109 (1998).
- [12] M. Post et al., *Nucl. Phys.* **A689**, 753 (2001).
- [13] J. Wambach, *Nucl. Phys.* **A715**, 422c (2003).
- [14] W. Cassing et al., *Phys.Lett.* **B363**, 35 (1995).
- [15] R. Rapp, J. Wambach, *Adv. Nucl. Phys.* **25**, 1 (2000).
- [16] R. Rapp, *Pramana* **60**, 675 (2003), hep-ph/0201101.
- [17] V. Koch et al., *Proc. Int. Workshop XXVIII on Gross Properties of Nuclei and Nuclear Excitations*, Hirschegg, Austria, Jan. 16-22, 2000, GSI Report ISSN 0720-8715.
- [18] T. Renk et al., *Phys. Rev.* **C66**, 014902 (2002).
- [19] J. Adams et al., STAR collaboration, *Phys. Rev. Lett.* **92**, 092301 (2004).
- [20] U. Mosel, *Proc. Int. Workshop XXV on Gross Properties of Nuclei and Nuclear Excitations*, Hirschegg, Austria, Jan. 13 - 18, 1997, p. 201, GSI Report ISSN 0720-8715.
- [21] U. Mosel, *Progr. Part. Nucl. Phys.* **42** 161 (1999)
- [22] U. Mosel, *Proc. Int. Workshop XXVIII on Gross Properties of Nuclei and Nuclear Excitations*, Hirschegg, Austria, Jan. 16-22, 2000, GSI Report ISSN 0720-8715.
- [23] M. Gyulassy et al., *Quark Gluon Plasma Vol. 3*, ed. R.C. Hwa and X.N. Wang, World Scientific, Singapore, 2003.
- [24] A. Airapetian et al., *Eur. Phys. J.* **C20**, 479; V. Muccifora et al., *Nucl. Phys.* **A711**, 254 (2002).
- [25] S. Zschocke, O.P. Pavlenko, B. Kaempfer, hep-ph/0212201.
- [26] E.L. Bratkovskaya, *Phys. Lett.* **B529**, 26 (2002).
- [27] T. Weidmann et al., *Phys. Rev.* **C59**, 919 (1999)
- [28] M. Effenberger et al., *Phys. Rev.* **C60**, 027601 (1999)
- [29] M. Effenberger, E.L. Bratkovskaya, U. Mosel, *Phys. Rev.* **C60**, 044614 (1999).
- [30] W. Cassing, E.L. Bratkovskaya, *Phys. Rep.* **308**, 65 (1999).
- [31] K. Shekhter et al., *Phys. Rev.* **C68** **2003** 014904



- [32] N. Bianchi et al., *Phys. Rev.* **C60** 064617 (1999).
- [33] M. Effenberger, U. Mosel, *Phys. Rev.* **C62**, 014605 (2000).
- [34] T. Falter, K. Gallmeister, U. Mosel, *Phys. Rev.* **C67** 054606 (2003), Erratum-ibid. **C68**, 019903 (2003).
- [35] T. Falter et al., *Phys. Rev.* **C70** 054609 (2004).
- [36] S. Leupold, *Nucl. Phys.* **A672** 475 (2000).
- [37] W. Cassing and S. Juchem, *Nucl. Phys.* **A665** (2000) 377
- [38] M. Roebig-Landau et al., *Phys. Lett.* **B373**, 421 (1997).
- [39] B. Krusche, private communication
- [40] T. Yorita et al., *Phys. Lett.* **B476** 226 (2000); H. Yamazaki et al., *Nucl. Phys.* **A670**, 202c (2000).
- [41] M. Effenberger et al., *Nucl. Phys.* **A613**, 353 (1997).
- [42] J. Lehr, M. Post, U. Mosel, *Phys. Rev.* **C68**, 044601 (2003).
- [43] J. Lehr and U. Mosel, *Phys. Rev.* **C68**, 044603 (2003).
- [44] F. Bonutti, *Nucl. Phys.* **A677**, 213 (2000).
- [45] J.G Messchendorp et al., *Phys. Rev. Lett.* **89**, 222302 (2002).
- [46] L. Roca, E. Oset and M.J. Vicente Vacas, *Phys. Lett.* **B541**, 77 (2002)
- [47] P. Mühlich et al., *Phys. Lett.* **B595**, 216 (2004)
- [48] J. G. Messchendorp et al., *Eur. Phys. J.* **A11**, 95 (2001).
- [49] F. Klingl, T. Waas, W. Weise, *Nucl. Phys.* **A650**, 299 (1999).
- [50] B. Friman, *Acta Phys. Polon.* **B29**, 3195 (1998).
- [51] P. Muehlich, T. Falter, U. Mosel, *Eur.Phys.J.* **A20**, 499 (2004).
- [52] G. E. Brown, M. Rho, *Phys. Rev. Lett.* **66**, 2720 (1991).
- [53] D. Trnka, V. Metag, private communication
- [54] R.J. Porter et al., *Phys. Rev. Lett.* **79**, 1229 (1997).
- [55] JLAB experiment E-01-112.
- [56] U. Mosel, *Proc. Int. Workshop XXIII on Gross Properties of Nuclei and Nuclear Excitations*, Hirschegg, Austria, Jan. 16 - 21, 1995, p. 184, GSI Report ISSN 0720-8715
- [57] W. K. Brooks, *Fizika* **B13**, 321-328 (2004).
- [58] E. Wang, X.-N. Wang, *Phys. Rev. Lett.* **89** 162301 (2002); F. Arleo, *Eur. Phys. J.* **C30**, 213 (2003).
- [59] A. Accardi, V. Muccifora, H.-J. Pirner, *Nucl. Phys.* **A720**, 131 (2003).

- [60] T. Falter et al., *Phys. Lett.* **B594**, 61-68 (2004)
- [61] B. Z. Kopeliovich et al., *Nucl. Phys.* **A740**, 211 (2004) .
- [62] C. Ciofi degli Atti, B. Z. Kopeliovich, *Eur. Phys. J.* **A17**, 133 (2003).
- [63] P. di Nezza et al., private communication
- [64] T. Falter, University of Giessen PhD thesis, 2004, <http://theorie.physik.uni-giessen.de/html/dissertations.ht>